

01,05,11

## First-principle studies of the tendency towards segregation in Heusler alloys $\text{Ni}_2\text{Mn}_{1+x}\text{Sb}_{1-x}$ with different atomic ordering

© K.R. Erager, V.V. Sokolovskiy, V.D. Buchelnikov

Chelyabinsk State University,  
Chelyabinsk, Russia

E-mail: eragerk@rambler.ru

Received July 8, 2021

Revised July 8, 2021

Accepted July 8, 2021

Using ab initio calculations, the stability issues of a series of Heusler alloys  $\text{Ni}_2\text{Mn}_{1+x}\text{Sb}_{1-x}$  ( $x = 0, 0.25, 0.5, 0.75, 1$ ) with staggered and layer-by-layer ordering of Mn atoms are investigated. It is shown that compositions with an excess of Mn are stable with respect to decomposition into constituent elements and unstable with respect to decomposition into a two-phase system consisting of a ferromagnetic cubic  $L2_1$ -phase  $\text{Ni}_2\text{MnSb}$  and an antiferromagnetic tetragonal  $L1_0$ -phase  $\text{NiMn}$ . Thus, all nonstoichiometric compositions in the austenite and martensitic phases, taking into account different magnetic and atomic ordering, tend to segregate. Stability of alloys is possible only in stoichiometric compositions ( $x = 0$  and  $1$ ).

**Keywords:** Heusler alloys, ab initio calculations, segregation, phase stability.

DOI: 10.21883/PSS.2022.13.52297.11s

### 1. Introduction

Today the perspectives of the Heusler alloys based on Ni and Mn are conditioned by the presence of a series of various functional properties [1–18], such as magnetocaloric effect [7–10], magnetoresistance [11,12], shape memory effect [9,13–15] and pinning [16–17]. A wide versatility of functional properties of these alloys is determined by the presence in them of magnetic, structural and associated magnetic-structural phase transformations. This is why intermetallic Heusler compounds represent a special interest, both from fundamental and application points of view.

Unlike the Ni-Mn-Ga family Ni-Mn-Z ( $Z = \text{In, Sn, Sb}$ ) alloy undergo martensite transformation only in non-stoichiometric compounds at certain ratios between Mn and Z [19–23]. As a result, occurrence of any functional properties is directly associated with the composition. Common specific of the Ni-Mn-Z alloy is the presence of confident ferromagnet (FM)-antiferromagnet (AFM) correlations between Mn atoms located in non-equivalent positions of the crystalline lattice. The most apparent FM-AFM correlations are in the low-temperature martensite phase, because Mn atoms are located at closer distances versus the same distances in the cubic austenite phase. As a result, the martensite phase has considerably lower magnetization intensity, and in the martensite transformation area there is stepwise variation of the magnetization intensity resulting in high values of reverse magnetocaloric effect and magnetoresistance [7–12].

It should be noted that in the vast majority of experimental works non-stoichiometric compositions were thermally treated by standard quenching methods and annealing

with duration over several days. Recent experimental studies [24–29] of impact of a long-term annealing to the phase stability of the Ni-Mn-(Ga, Sn, In Al) alloys with high content of Mn have shown the following: two-step annealing during 4 weeks at the temperature of  $\approx 1200$  K and during 1 week at the temperature of about 770 K result in disappearing of the martensite transformation and segregation into two-phase system consisting of the FM matrix  $\text{Ni}_2\text{Mn}(\text{Ga, Sn, In, Al})$  with cubic structure and AFM tetragonal phase  $\text{NiMn}$ .

Regarding the Ni-Mn-Sb family alloys, these compounds are less studied under experimental and theoretical approaches. Nevertheless, the works [30,31] presented studies of the composition phase diagrams of  $\text{Ni}_2\text{Mn}_{1+x}\text{Sb}_{1-x}$  alloys, according to which there is a complex sequence of magnetic and structural phase transformation with deviation from stoichiometry ( $x > 0.3$ ). At the same time the martensite transformation and the properties associated therewith are highly sensitive to the ratio of concentrations between Ni, Mn and Sb. A series of the works [32,33] studied magnetocaloric and transport properties in the area of martensite transformation demonstrating similar results for the Ni-Mn-(In, Sn) alloys. Theoretical studies from the first principles [34–36] also show sensitivity of magnetic and structural properties of austenite and martensite phases of the Ni-Mn-Sb alloys to the change of chemical composition and degree of filling the crystallographic positions. However, the issues of phase stability of that alloys were considered poorly.

Herein we present the studies of stability of magnetic and crystalline structure of austenite and martensite phases of  $\text{Ni}_2\text{Mn}_{1+x}\text{Sb}_{1-x}$  alloys within the framework of the density functional theory.

## 2. Details and methodology of analysis

The first principle analysis of properties of the  $\text{Ni}_2\text{Mn}_{1+x}\text{Sb}_{1-x}$  alloys is made by using the Projector Augmented Wave method (PAW) implemented in the VASP software package [37,39]. To describe the exchange-correlation energy a generalized gradient approximation in parametrization of Perdew–Burke–Ernzerhof was selected [39]. Brillouin zone integration was done by Monkhorst–Pack method, by using  $k$ -point grid  $12 \times 12 \times 12$ . The plane waves energy cutoff of 450 eV, and the energy convergence parameter was  $10^{-8}$  eV/atom. The following electron configurations were selected as PAW of pseudopotentials:  $3p^6 4s^1 3d^7$  for Mn,  $3p^6 4s^2 3d^8$  for Ni and  $5p^3 5s^2$  for Sb. Geometric optimization of crystalline structures of austenite and martensite phases is made within the framework of electron and ion relaxation. The crystalline structure of austenite phase is specified by 16-atom cubical supercell of the spatial group of symmetry #225. Non-stoichiometric compositions  $\text{Ni}_2\text{Mn}_{1+x}\text{Sb}_{1-x}$  ( $x = 0.25, 0.5$  and  $0.75$ ) are formed by allocating one, two and three excessive Mn atoms at the positions of Sb.

Since the Heusler alloys with excess of Mn demonstrate a complicated behavior in long-acting exchange interactions, especially in the martensite phase, then it is necessary to consider different magnetic structures. This work deals with two cases of alignment of magnetic moments of Mn and Ni atoms: ferromagnetic — FM (all spins  $\uparrow\uparrow$ ) and ferrimagnetic — FIM (spins of excessive Mn  $\downarrow\downarrow$ ). Fig. 1 shows cubical structures of compounds  $\text{Ni}_2\text{Mn}_{1+x}\text{Sb}_{1-x}$  ( $x = 0, 0.25, 0.5, 0.75, 1$ ) with allocation of Mn atoms in „staggered“ and in „layered“ order. The structure with layered atom alignment is a result of the presence of antisite defect between one couple of Mn and Sb atoms. Additionally the defect structure is considered, as described by authors of the work [36], with partial allocation of excessive Mn atoms in the positions of Ni.

By taking into account the experimental data [24–29], this work studied possible effects of segregation of Ni–Mn–Sb alloys resulting in occurrence of two-phase composites with FM cubical stoichiometric phase  $\text{Ni}_2\text{MnSb}$  and AFM tetragonal phase  $\text{NiMn}$ . Our methodology consists of three stages. At the first step we calculated the energies of main state subject to beneficial magnetic configuration both for stoichiometric and non-stoichiometric compounds. The second step is the analysis of stability of the compounds relative to decomposition into component elements within the framework of the formation energy (or enthalpy) calculations. The third step is the analysis of stability of compounds relative to decomposition into  $\text{Ni}_2\text{MnSb}$  and  $\text{NiMn}$  within the framework of the mixing energy calculations.

$$E_{\text{mix}} = E_{\text{Ni}_2\text{Mn}_{1+x}\text{Sb}_{1-x}} - \left[ (1-x)E_{\text{Ni}_2\text{MnSb}}^{L2_1} + xE_{(\text{NiMn})_2}^{L1_0} \right], \quad (1)$$

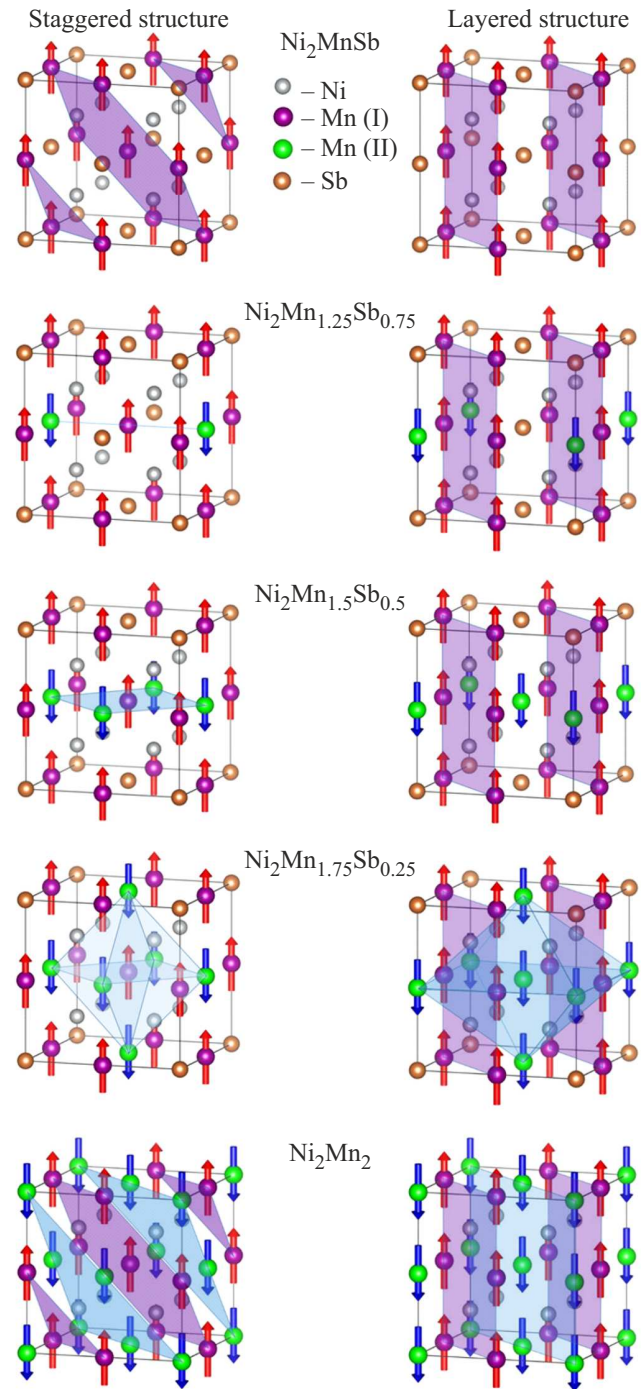


**Figure 1.** Cubical structures of compounds  $\text{Ni}_2\text{Mn}_{1+x}\text{Sb}_{1-x}$  ( $x = 0, 0.25, 0.5, 0.75, 1$ ) with staggered and layered arrangement of Mn atoms forming FIM-order. Mn atoms replacing Sb are indicated green. Shaded areas are presented to highlight atomic and magnetic arrangement.

where  $E_{\text{Ni}_2\text{Mn}_{1+x}\text{Sb}_{1-x}}$  is the total energy of corresponding compounds with the structure of austenite and martensite;  $E_{\text{Ni}_2\text{MnSb}}^{L2_1}$  and  $E_{(\text{NiMn})_2}^{L1_0}$  is the total energies of stoichiometric ternary and binary compounds with the structure  $L2_1$  and  $L1_0$ .

**Table 1.** Equilibrium values of parameters of the lattices of austenite and martensite phase, degree of tetragonal distortion ( $c/a$ ) and the crystal energy difference relative to the most stable phases ( $\Delta E$ ) for each of the compositions  $\text{Ni}_2\text{Mn}_{1+x}\text{Sb}_{1-x}$  subject to different magnetic and atomic arrangement

Composition		$c/a$	$a$ (Å)	$b$ (Å)	$c$ (Å)	$\Delta E$ (meV/atom)	
$\text{Ni}_2\text{MnSb}$	FM	Staggered	1	6.070	6.070	6.070	0
	FIM	Layered	1.35	5.450	5.450	7.433	4.424
$\text{Ni}_2\text{Mn}_{1.25}\text{Sb}_{0.75}$ FIM	Staggered	1	5.989	5.989	5.989	0	
		1.25	5.529	5.528	7.023	0.257	
	Layered	1.3	5.366	5.366	7.378	47.169	
	Ref [36]	1	5.992	5.992	5.992	53.336	
		1.3	5.481	5.479	7.109	42.802	
$\text{Ni}_2\text{Mn}_{1.5}\text{Sb}_{0.5}$ FIM	Staggered	1	5.932	5.932	5.945	17.591	
		1.35	5.343	5.343	7.200	0	
	Layered	1.35	5.269	5.269	7.339	36.552	
	Ref [36]	1.35	5.305	5.305	7.259	45.727	
$\text{Ni}_2\text{Mn}_{1.75}\text{Sb}_{0.25}$ FIM	Staggered	1	5.867	5.867	5.867	48.990	
		1.35	5.247	5.247	7.168	0	
	Layered	1.35	5.240	5.240	7.167	10.982	
	Ref [36]	1.4	5.219	5.210	7.225	44.869	
$\text{Ni}_2\text{Mn}_2$ FIM	Staggered	1.41	5.094	5.094	7.223	60.261	
	Layered	1.41	5.125	5.125	7.166	0	

**Table 2.** Equilibrium values of total and element-by-element magnetic moments in austenite and martensite phases of  $\text{Ni}_2\text{Mn}_{1+x}\text{Sb}_{1-x}$  alloys subject to different magnetic and atomic arrangement

Composition			$c/a$	$M_A$ ( $\mu_B/\text{f.u.}$ )				
				Ni	Mn(I)	Mn(II)	Sb	Total
$\text{Ni}_2\text{MnSb}$	FM	Staggered	1	0.165	3.439	–	–0.020	3.748
	FIM	Layered	1.35	0	3.112	–3.112	–0.068	0
$\text{Ni}_2\text{Mn}_{1.25}\text{Sb}_{0.75}$ FIM	Staggered	1	0.107	3.358	–3.455	–0.029	2.686	
		1.25	0.219	3.268	–3.325	–0.046	2.841	
	Layered	1.3	0.167	3.007	–3.228	–0.084	2.470	
	Ref [36]	1	0.152	3.308	–2.765	–0.008	2.916	
		1.3	0.217	3.155	–2.821	–0.034	2.858	
$\text{Ni}_2\text{Mn}_{1.5}\text{Sb}_{0.5}$ FIM	Staggered	1	0.049	3.286	–3.424	–0.040	1.652	
		1.35	0.017	3.072	–3.198	–0.078	1.459	
	Layered	1.35	0.039	2.916	–3.119	–0.090	1.389	
	Ref [36]	1.35	0.027	2.945	–3.048	–0.060	1.440	
$\text{Ni}_2\text{Mn}_{1.75}\text{Sb}_{0.25}$ FIM	Staggered	1	0.014	3.240	–3.376	–0.050	0.723	
		1.35	0.066	3.045	–3.115	–0.074	0.824	
	Layered	1.35	0.088	2.998	–3.042	–0.071	0.877	
	Ref [36]	1.4	0.031	2.912	–3.017	–0.064	0.694	
NiMn FIM	Staggered	1.41	0	3.027	–3.027	–	0	
	Layered	1.41	0	3.158	–3.158	–	0	

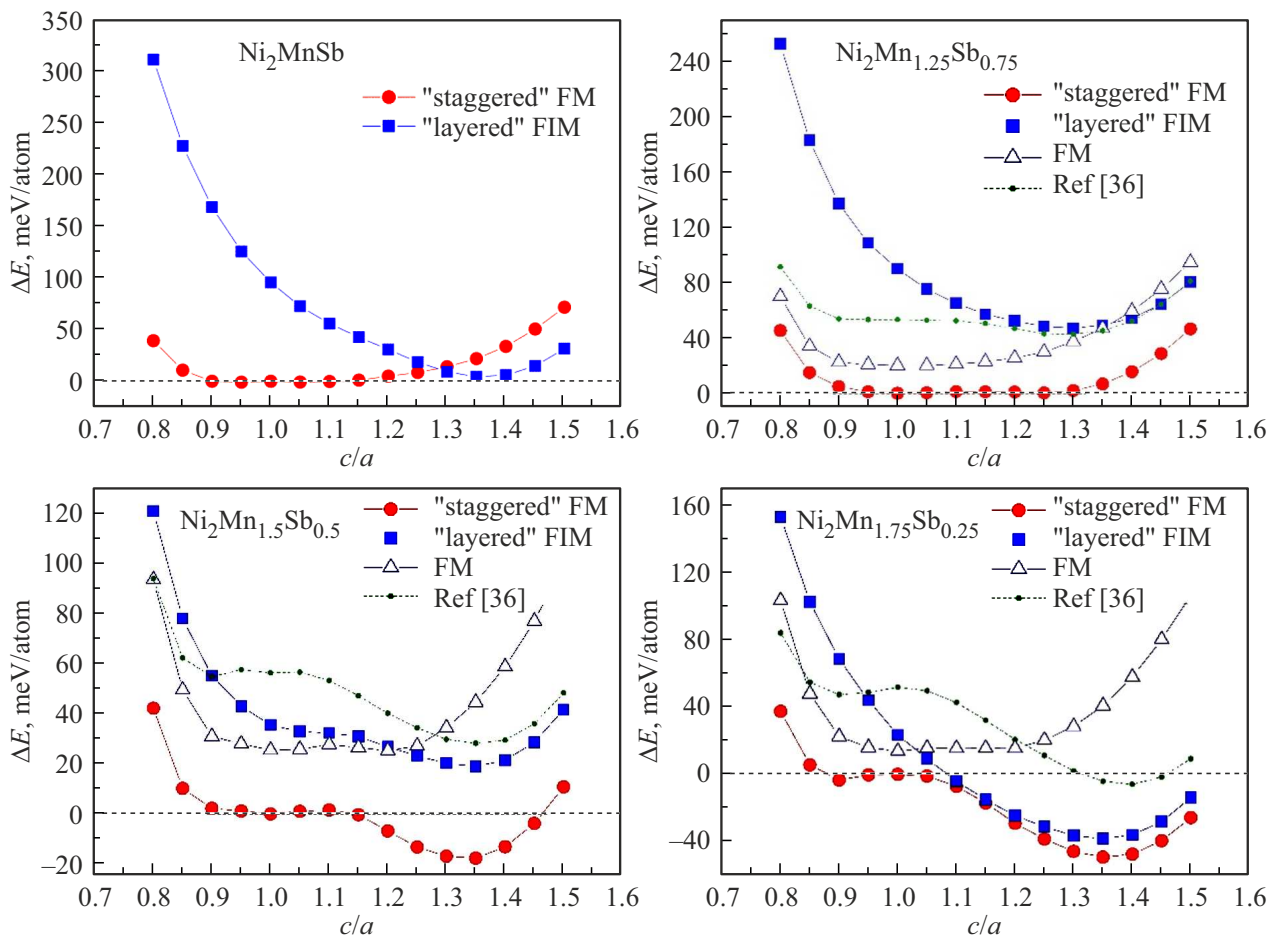


**Figure 2.** Dependence of the crystal energy difference on tetragonal distortion in the systems  $\text{Ni}_2\text{Mn}_{1+x}\text{Sb}_{1-x}$  ( $x = 0, 0.25, 0.5, 0.75$ ) with „staggered“ and „layered“ arrangement subject to FM- and FIM-order. Additionally, the results of analysis for defective structures in non-stoichiometric compositions are provided as proposed in the work [36].

### 3. Results of analyses and discussion

Proceed with the discussion of the obtained results of calculations of the energy of main state in cubic austenite and tetragonal martensite phases. Fig. 2 shows dependencies of the energy difference on tetragonal distortion ( $c/a$ ) for the systems  $\text{Ni}_2\text{Mn}_{1+x}\text{Sb}_{1-x}$  ( $x = 0, 0.25, 0.5, 0.75$ ) with staggered and layered arrangement of Mn, forming FM- and FIM-order. The difference of energies is taken relative to the austenite phase ( $c/a = 1$ ) with staggered arrangement of Mn.

Consider the results for stoichiometric composition of  $\text{Ni}_2\text{MnSb}$ . The calculations show that the staggered arrangement of Mn atoms stabilizes austenite  $L2_1$ -phase, also there is no martensite phase due to its impracticality. Otherwise, layered arrangement of Mn atoms results in occurrence of metastable martensite phase with tetragonal ratio  $c/a = 1.35$ . Notably, the martensite phase with layered arrangement is close in terms of the energy to the austenite phase with staggered arrangement ( $\Delta E \approx 4.424$  meV/atom). In case of non-stoichiometric compositions FIM staggered arrangement of Mn atoms becomes far more beneficial

in terms of the energy both for austenite and martensite phases. Moreover, for the composition  $\text{Ni}_2\text{Mn}_{1.25}\text{Sb}_{0.75}$  one may observe virtually degenerated state of austenite phase due to the minimum difference between the energies of cubical and tetragonal phases ( $\Delta E \approx 0.257$  meV/atom). Further increase of Mn content results in increase of the energy difference between austenite and martensite phases for the structures with staggered atomic arrangement, which indirectly indicates increase of the martensite transformation temperature. Such trend has a good coincidence with the experimental observations [31,40,41], according to which the temperature of martensite transformation  $T_M$  rises as far as the the Sb concentration falls down. Accounting of allocation of excessive Mn atoms in the positions of Ni and Sb similar to the work [36] results in increase of the energy of austenite and martensite phases approximately by 40 meV/atom. Moreover, as can be seen in Figure, for the composition  $\text{Ni}_2\text{Mn}_{1.75}\text{Sb}_{0.25}$  the energy of austenite phase, in which excessive Mn atoms are fully allocated in the Sb sublattice, is almost equal to the energy of martensite phase, in which excessive Mn atoms occupy the positions

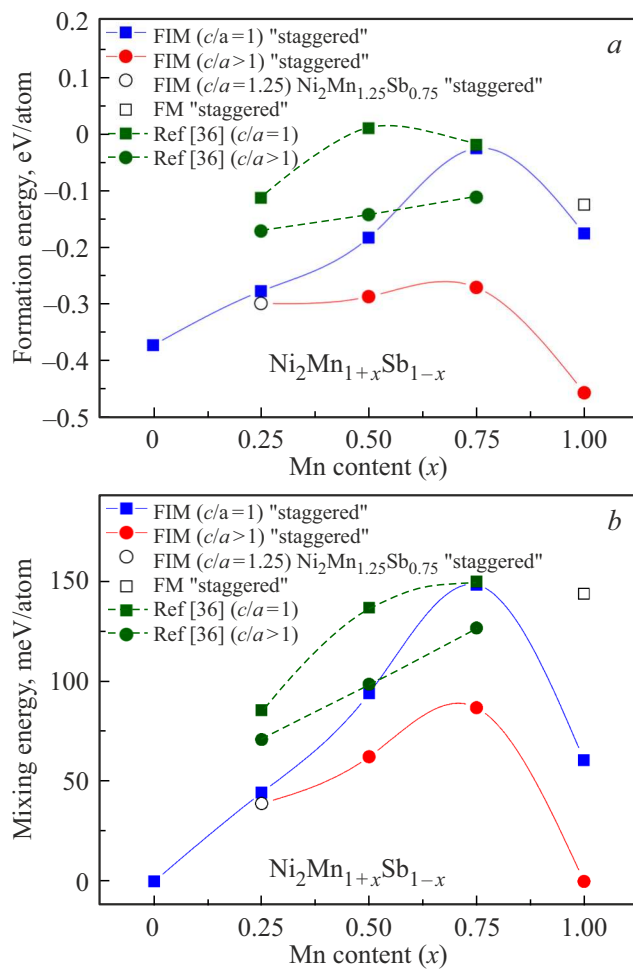


**Figure 3.** Dependence of the energy (a) of formation and (b) mixing on the Mn content for cubical  $L_{21}$  and tetragonal  $L_{10}$ -phase of  $\text{Ni}_2\text{Mn}_{1+x}\text{Sb}_{1-x}$  alloys subject to different magnetic and atomic arrangement.

of Ni and Sb. This observation also indicates degradation of the austenite phase depending on the degree of filling of crystallographic positions.

Table 1 shows equilibrium parameters of the lattice for the alloys  $\text{Ni}_2\text{Mn}_{1+x}\text{Sb}_{1-x}$  in austenite and martensite phase subject to different atomic and magnetic arrangement. It is established, that as far as Mn content is increased, the constants of lattices of both phases fall down, which can be explained by less atomic radius of Mn (1.40 Å) versus Sb (1.45 Å). The calculated values correlate with the experimental data [31] and theoretical studies of other authors [36].

Table 2 shows the values of total and element-by-element magnetic moments for the compounds under study. The highest value of total magnetic moment is observed for stoichiometric composition subject to staggered arrangement of Mn atoms. Further decrease of Sb concentration results in decrease of the magnetic moment value in the austenite and martensite phases with staggered and layered FIM arrangement. The observed trend in behavior

of magnetization intensity has a good correlation with the experiment [31]. AFM-arrangement is observed for stoichiometric compounds  $\text{Ni}_2\text{MnSb}$  with layered atomic arrangement and NiMn with staggered and layered atomic arrangement.

Fig. 3, a shows dependencies of the formation energy on the Mn concentration for austenite and martensite phase of the studied compositions, which are ferro-, antiferro-, and ferrimagnetic arranged. According to Figure all compositions are stable relative to decomposition into component elements, because the formation energy takes negative values and its magnitude modulus rises as far as the Mn content is increased. However, if consider more complex decomposition products observed experimentally [24–29], one can see an opposite trend (Fig. 3, b). All non-stoichiometric compositions in austenite and martensite phase with different atomic and magnetic arrangement appear to be instable because of the positive mixing energy value, i.e. single phase in such compounds under equilibrium conditions could remain disputable. It should be noted, that Mn-rich Heusler alloys feature strong competing ferro- and antiferromagnetic exchange interactions, which are long-range and oscillating. Therefore, the higher is the content of excessive Mn atoms in the Sb sublattice, the heavier is such competition. According to Fig. 3, b, the mixing energy, as well as its difference for austenite and martensite phase, is increased for all compositions with decrease of Sb content, thus confirming the trend to segregation into FM cubical  $L_{21}$  phase  $\text{Ni}_2\text{MnSb}$  and AFM tetragonal  $L_{10}$  phase NiMn. Stable are only stoichiometric compounds  $\text{Ni}_2\text{MnSb}$  and NiMn.

## 4. Conclusion

This work presented the studies of magnetic and structural properties of Heusler alloys  $\text{Ni}_2\text{Mn}_{1+x}\text{Sb}_{1-x}$  depending on the atomic and magnetic arrangement. It is shown that for all non-stoichiometric compositions the most beneficial arrangement in terms of the energy is ferrimagnetic staggered arrangement of Mn atoms, meanwhile the martensite transformation is possible for the compositions  $x > 0.25$ . Otherwise, layered arrangement of Mn atoms for each composition results in occurrence of martensite phase only. It was found that in stoichiometry the cubic phase with staggered atomic arrangement and tetragonal phase with layered arrangement of Mn atoms are similar in terms of the energy, the difference with more beneficial cubical phase is about 4.424 meV/atom, which indicates possible degradation of austenite phase and its multi-phase nature. The study of trends to segregation of alloys with excessive content of manganese in austenite and martensite phase subject to different magnetic and atomic arrangement, shows their instability to decomposition into double-phase system, consisting of three-component stoichiometric compound of the cubic phase  $L_{21}$  and binary compound of the tetragonal

phase  $L1_0$ . Stability is demonstrated only by stoichiometric compounds  $Ni_2MnSb$  and  $NiMn$ .

## Acknowledgments

Calculations of structures with staggered atoms arrangement were done with the project support from the Russian Science Foundation No. 17-72-20022. Calculations of structures with layered atoms arrangement were done with the support from the Ministry of Science and Higher Education of the Russian Federation within the framework of state assignment No. 075-00992-21-00.

## Conflict of interest

The authors declare that they have no conflict of interest.

## References

- [1] K. Ullakko, J. Huang, C. Kantner, R. O'Handley, V. Kokorin. *Appl. Phys. Lett.* **69**, 1966 (1996).
- [2] S.J. Murray, M. Marioni, S. Allen, R. O'Handley, T.A. Lograsso. *Appl. Phys. Lett.* **77**, 886 (2000).
- [3] A. Sozinov, A. Likhachev, N. Lanska, K. Ullakko. *Appl. Phys. Lett.* **80**, 1746 (2002).
- [4] M. Chmielus, X. Zhang, C. Witherspoon, D. Dunand, P. Müllner. *Nature Mater.* **8**, 863 (2009).
- [5] J. Marcos, A. Planes, L. Mañosa, F. Casanova, X. Batlle, A. Labarta, B. Martínez. *Phys. Rev. B* **66**, 224413 (2002).
- [6] F.-X. Hu, B.-G. Shen, J.-R. Sun, G.-H. Wu. *Phys. Rev. B* **64**, 132412 (2001).
- [7] T. Krenke, E. Duman, M. Acet, E.F. Wassermann, X. Moya, L. Mañosa, A. Planes, E. Suard, B. Ouladdiaf. *Phys. Rev. B* **75**, 104414 (2007).
- [8] M. Pasquale, C.P. Sasso, L.H. Lewis, L. Giudici, T. Lograsso, D. Schlögl. *Phys. Rev. B* **72**, 094435 (2005).
- [9] A.P. Kamantsev, Yu.S. Koshkidko, E.O. Bykov, V.S. Kalashnikov, A.V. Koshelev, A.V. Mashirov, I.I. Musabirov, M.A. Paukov, V.V. Sokolovskiy. *FTT* **62**, 727 (2020).
- [10] O.N. Miroshkina, V.V. Sokolovskiy, M.A. Zagrebina, S.V. Taskaev, V.D. Buchelnikov. *FTT* **62**, 697 (2020).
- [11] C. Biswas, R. Rawat, S. Barman. *Appl. Phys. Lett.* **86**, 202508 (2005).
- [12] V. Sharma, M. Chattopadhyay, K. Shaeb, A. Chouhan, S. Roy. *Appl. Phys. Lett.* **89**, 222509 (2006).
- [13] R. Kainuma, Y. Imano, W. Ito, Y. Sutou, H. Morito, S. Okamoto, O. Kitakami, K. Oikawa, A. Fujita, T. Kanomata, K. Ishida. *Nature* **439**, 957 (2006).
- [14] R. Kainuma, Y. Imano, W. Ito, H. Morito, Y. Sutou, K. Oikawa, A. Fujita, K. Ishida, S. Okamoto, O. Kitakami, T. Kanomata. *Appl. Phys. Lett.* **88**, 192513 (2006).
- [15] V. Khovaylo, K. Skokov, O. Gutfleisch, H. Miki, R. Kainuma, T. Kanomata. *Appl. Phys. Lett.* **97**, 052503 (2010).
- [16] Z. Li, C. Jing, J. Chen, S. Yuan, S. Cao, J. Zhang. *Appl. Phys. Lett.* **91**, 112505 (2007).
- [17] M. Khan, I. Dubenko, S. Stadler, N. Ali. *Appl. Phys. Lett.* **91**, 072510 (2007).
- [18] O.N. Miroshkina, M.A. Zagrebina, V.V. Sokolovskiy, V.D. Buchelnikov. *FTT* **60**, 1127 (2018).
- [19] K. Koyama, H. Okada, K. Watanabe, T. Kanomata, R. Kainuma, W. Ito, K. Oikawa, K. Ishida. *Appl. Phys. Lett.* **89**, 182510 (2006).
- [20] S. Yu, Z. Liu, G. Liu, J. Chen, Z. Cao, G. Wu, B. Zhang, X. Zhang. *Appl. Phys. Lett.* **89**, 162503 (2006).
- [21] M.K. Ray, B. Maji, M. Modak, S. Banerjee. *J. Magn. Magn. Mater.* **429**, 110 (2017).
- [22] N.V. Rama Rao, R. Gopalan, V. Chandrasekaran, K.G. Suresh. *Appl. Phys. A* **99**, 265 (2010).
- [23] Z. Han, D. Wang, C. Zhang, H. Xuan, B. Gu, Y. Du. *Appl. Phys. Lett.* **90**, 042507 (2007).
- [24] W.M. Yuhasz, D.L. Schlögl, Q. Xing, K.W. Dennis, R.W. McCallum, T.A. Lograsso. *J. Appl. Phys.* **105**, 07A921 (2009).
- [25] W.M. Yuhasz, D.L. Schlögl, Q. Xing, R.W. McCallum, T.A. Lograsso. *J. Alloys Compd.* **492**, 681 (2010).
- [26] T. Krenke, A. Çakir, F. Scheibel, M. Acet, M. Farle. *J. Appl. Phys.* **120**, 243904 (2016).
- [27] A. Çakir, M. Acet, M. Farle. *Sci. Rep.* **6**, 28931 (2016).
- [28] A. Çakir, M. Acet. *AIP Adv.* **7**, 056424 (2017).
- [29] A. Çakir, M. Acet, U. Wiedwald, T. Krenke, M. Farle. *Acta Mater.* **127**, 117 (2017).
- [30] Y. Sutou, Y. Imano, N. Koeda, T. Omori, R. Kainuma, K. Ishida, K. Oikawa. *Appl. Phys.* **85**, 4358 (2004).
- [31] M. Khan, I. Dubenko, S. Stadler, N. Ali. *J. Phys.: Condens. Matter* **20**, 235204 (2008).
- [32] W.J. Feng, Q. Zhang, L.Q. Zhang, B. Li, J. Du, Y.F. Deng, Z.D. Zhang. *Solid State Commun.* **150**, 949 (2010).
- [33] B. Kwon, Y. Sakuraba, H. Sukegawa, S. Li, G. Qu, T. Furubayashi, K. Hono. *J. Appl. Phys.* **119**, 023902 (2016).
- [34] J. Rusz, L. Bergqvist, J. Kudrnovský, I. Turek. *Phys. Rev. B* **73**, 214412 (2006).
- [35] J. Rusz, J. Kudrnovský, I. Turek. *J. Magn. Magn. Mater.* **310**, 1654 (2007).
- [36] S. Ghosh, S. Ghosh. *Phys. Rev. B* **99**, 064112 (2019).
- [37] G. Kresse, J. Furthmüller. *Phys. Rev. B* **54**, 11169 (1996).
- [38] G. Kresse, D. Joubert. *Phys. Rev. B* **59**, 1758 (1999).
- [39] J.P. Perdew, K. Burke, M. Ernzerhof. *Phys. Rev. Lett.* **77**, 3865 (1996).
- [40] M. Khan, N. Ali, S. Stadler. *J. Appl. Phys.* **101**, 053919 (2007).
- [41] W.J. Feng, J. Du, B. Li, W.J. Hu, Z.D. Zhang, X.H. Li, Y.F. Deng. *J. Phys. D* **42**, 125003 (2009).